UV-C irradiation is highly effective in inactivating SARS-CoV-2 replication

Mara Biasin[1], Andrea Bianco[2], Giovanni Pareschi[2], Adalberto Cavalleri[3], Claudia Cavatorta[3], Claudio Fenizia[1,6], Paola Galli[2], Luigi Lessio[4], Manuela Lualdi[5], Enrico Tombetti[1], Alessandro Ambrosi[6], Edoardo Maria Alberto Redaelli[2], Irma Saulle[1,7], Daria Trabattoni[1], Alessio Zanutta[2], Mario Clerici[7,8,*]

[1] Department of Biomedical and Clinical Sciences L. Sacco, University of Milano, Milano, Italy.
[2]Italian National Institute for Astrophysics (INAF) – Brera Astronomical Observatory, Merate, Italy.
[3] Epidemiology and Prevention Unit, IRCCS Foundation, Istituto Nazionale dei Tumori, Milan, Italy.
[4] Italian National Institute for Astrophysics (INAF) – Padova Astronomical Observatory, Padova, Italy.
[5] Department of Imaging Diagnostic and Radioterapy, IRCCS Foundation, Istituto Nazionale dei Tumori, Milan, Italy.
[6] University Life and health San Raffaele, Milan, Italy.
[7] Department of Pathophysiology and Transplantation, University of Milano, Milano, Italy.
[8]Don C. Gnocchi Foundation, IRCCS Foundation, Milano, Italy.

The potential virucidal effects of UV-C irradiation on SARS-CoV-2 were experimentally evaluated for different illumination doses and virus concentrations (1000, 5, 0.05 MOI). At a virus density comparable to that observed in SARS-CoV-2 infection, an UV-C dose of just 3.7 mJ/cm^2 was sufficient to achieve a more than 3-log inactivation without any sign of viral replication. Moreover, a complete inactivation at all viral concentrations was observed with 16.9 mJ/cm^2. These results could explain the epidemiological trends of COVID-19 and are important for the development of novel sterilizing methods to contain SARS-CoV-2 infection.

Introduction

The COVID-19 pandemic caused by SARS-CoV-2 virus[1] has had an enormous, as yet barely understood, impact on health and economic outlook at the global level[2]. The identification of effective microbicide approaches is of paramount importance in order to limit further viral spread, as the virus can be transmitted via aerosol[3,4] and can survive for hours outside the body[5–7]. Non-contact disinfection technologies are highly desirable, and UV radiation, in particular UV-C (200 – 280 nm) has been suggested to be able to inactivate different viruses, including SARS-CoV[8–12]. The interaction of UV-C radiations with viruses has been extensively studied[13–15], and direct absorption of the UV-C photon by the nucleic acid basis and/or capsid proteins leading to the generation of photoproducts that inactivate the virus was suggested

* e-mail: mario.clerici@unimi.it

34 to be one of the main UV-C-associated virucidal mechanisms[16,17]. Some models have been proposed to
35 correlate the nucleic acid structure with the required dose to inactivate the virus, but a reliable model is
36 still unavailable[18]. This is also due to the fact that UV-C measurements were conducted using different
37 viruses and diverse experimental conditions[19–22]. This led to an extremely wide range of values for the same
38 virus and, e.g., in the case of SARS-CoV-1 values reported in the literature range from a few mJ/cm^2 to
39 hundreds mJ/cm^2 [19,22,23]. Likewise, recent papers reported values for UVC inactivation ranging from 3 to
40 1000 mJ/cm^2 [24–27]. A better understanding of the effects of UV-C on SARS-CoV-2 , which take into account
41 all the key factors involved in the experimental setting (including culture medium, SARS-CoV-2
42 concentration, UV-C irradiance, time of exposure, and UV-C absorbance) will allow to replicate the results
43 in other laboratory with different devices. Moreover, as recent evidences suggest that UV light from
44 sunlight are efficient in inactivating the virus[28], these measurements will be relevant for the setting up of
45 further experiment considering the role of UV-A and UV-B on SARS-CoV-2 replication.
46
47 **Results and discussion**
48 Herein, we report the effect of monochromatic UV-C (254 nm) on SARS-CoV-2, showing that virus
49 inactivation can be easily achieved. Experiments were conducted using a custom-designed low-pressure
50 mercury lamp system, which has been spectral-calibrated providing an average intensity of 1.082 mW/cm^2
51 over the illumination area (see the details reported in the Method section). Three different illumination
52 exposure times, corresponding to 3.7, 16.9 and 84.4 mJ/cm^2, were administered to SARS-CoV-2 either at a
53 multiplicity of infection (MOI) of 0.05, 5, 1000. The first concentration is equivalent to the low-level
54 contamination observed in closed environments (e.g. hospital rooms), the second one corresponds to the
55 average concentration found in the sputum of COVID-19 infected patients, and the third one is a very large
56 concentration, corresponding to that observed in terminally diseased COVID-19 patients[29] . After UV-C
57 exposure, viral replication was assessed by culture-polymerase chain reaction (C-RT-PCR) targeting two
58 regions (N1 and N2) of the SARS-CoV-2 nucleocapsid gene, as well as by analyzing SARS-CoV-2-induced
59 cytopathic effect. Analyses were performed in the culture supernatant of infected cells at three different
60 time points (24, 48 and 72 hours for SARS-CoV-2 at MOI 1000 and 5; 24, 48 hours and 6 days for SARS-CoV-

61 2 at MOI 0.05), as well as on cell lysates at the end of cellular culture (72 hours: MOI 1000 and 5; 6 days:
62 MOI 0.05). This approach allows to follow the kinetic of viral growth and to verify whether the used dose is
63 sufficient to completely inactivate the virus over time. This is useful from a practical point of view, when
64 UV-C devices are used to disinfect surfaces and the environment.
65 The effect of the UV-C exposure on SARS-CoV-2 replication was extremely evident and independent from
66 the MOI employed; dose-response and time-dependent curves were observed. Figure 1, 2 and 3 report for
67 different MOI the number of SARS-CoV-2 copies for the three concentrations as a function of the UV-C dose
68 and time, quantified on a standard curve from a plasmid control. The corresponding normalised curves of
69 the virus copies are reported in the same figures.

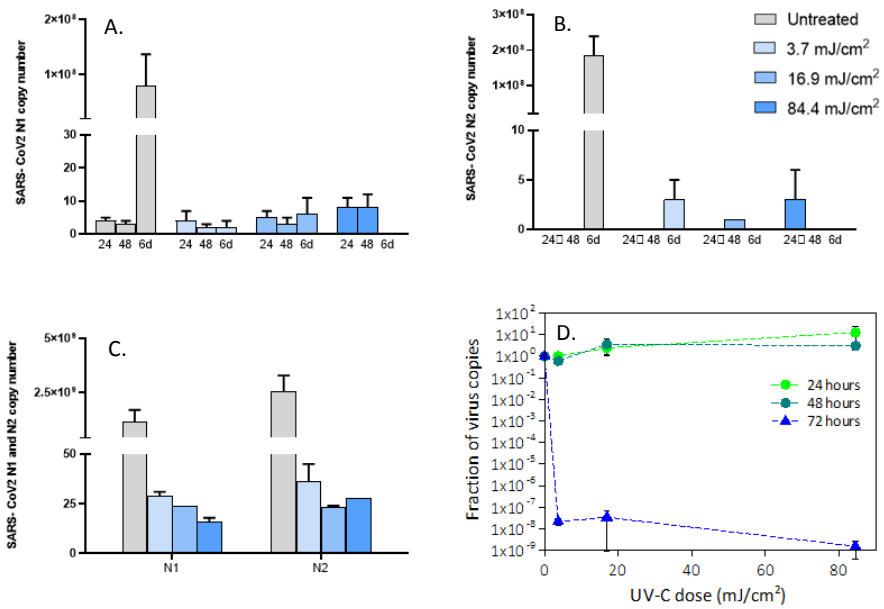

70
71 **Figure 1. Viral replication of UV-irradiated SARS-CoV-2 (0.05 MOI) virus in in vitro VeroE6 cells**. Vero E6 cells were infected with
72 UV-C irradiated SARS-CoV-2 virus at a MOI of 0.05. Culture supernatants were harvested at the indicated times (24, 48 hours and 6
73 days) and virus titers were measured (Panel A, B) by absolute copy number quantification (Real-Time PCR). Viral replication was
74 assessed even on cell lysate harvested at the end of cell cultures (6 days) (Panel C). All cell culture conditions were seeded in
75 duplicate. Panel D reports the plots of the measured virus copies normalized at the untreated sample in the different conditions.
76 For descriptive purposes, mean values and whiskers representing the observed half-ranges are shown.
77
78 Viral replication was not observed at the lowest viral concentration (0.05 MOI) in either untreated or in UV-
79 C-irradiated samples in the initial 48 hours (Figure 1). However, 6 days after infection, viral replication was
80 distinctly evident in the UV-C unexposed condition, but was completely absent following UV-C irradiation

81 even at 3.7 mJ/cm^2 both in cell culture supernatants (Figure1, panel A and B) and in cell lysate (Figure 1,

82 panel C). A two-way ANOVA analysing the effect of UV-C dose and time of incubation failed to identify a

83 significant effect of the UV exposure on viral replication. This is due to the fact that at very low MOI

84 relevant increases in N1 and N2 copy numbers were detectable only in a single condition -at six days in the

85 absence of UV-C exposure- thus hampering the statistical power of the analysis.

86

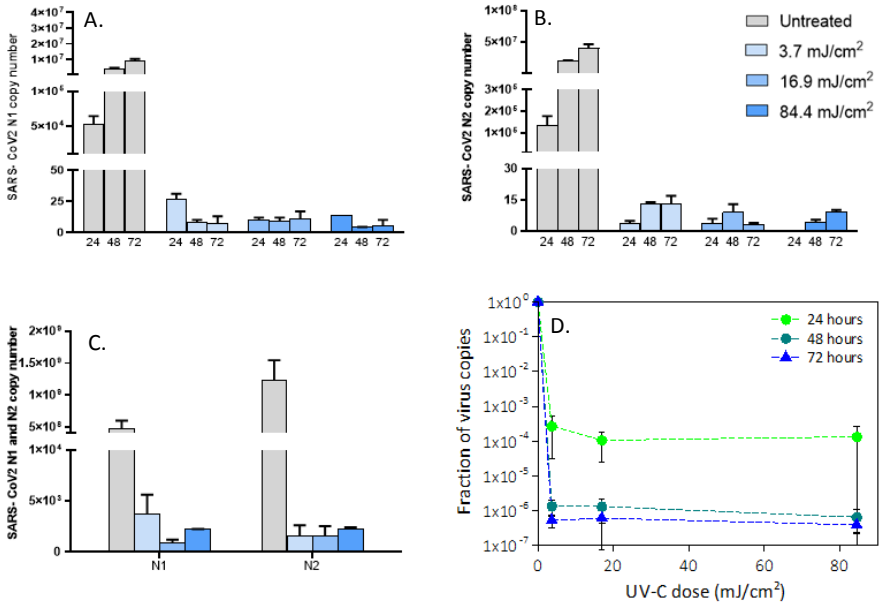

87

88 **Figure 2. Viral replication of UV-irradiated SARS-CoV-2 (5 MOI) virus in in vitro VeroE6 cells.** Vero E6 cells were infected with UV-C

89 irradiated SARS-CoV-2 virus at a MOI of 5. Culture supernatants were harvested at the indicated times (24, 48 and 72 hours) and

90 virus titers were measured by absolute copy number quantification (Real-Time PCR, A and B). Viral replication was assessed even

91 on cell lysate harvested at the end of cell cultures (72 hours) (C). All cell culture conditions were seeded in duplicate. Panel D

92 reports the plots of the measured virus copies normalized at the untreated sample in the different conditions. For descriptive

93 purposes, mean values and whiskers representing the observed half-ranges are shown.

94

95 At the intermediate viral concentration (5 MOI), a significant reduction of copy number starting from the

96 3.7 mJ/cm^2 dose with a decrease of a factor of 2000 (> 3-log decrease) after 24 hours was observed (Figure

97 2, panel D). A two-way ANOVA confirmed that this UV-C dose significantly dampened viral replication

98 (p=0.000796, and P=0.000713 for N1 and N2 copies respectively). Even more important, the copy number

99 did not increase over time, suggesting an effective inactivation of the virus, which was further confirmed by

100 cytopathic effect assessment (Figure 3, panel A, B and C).

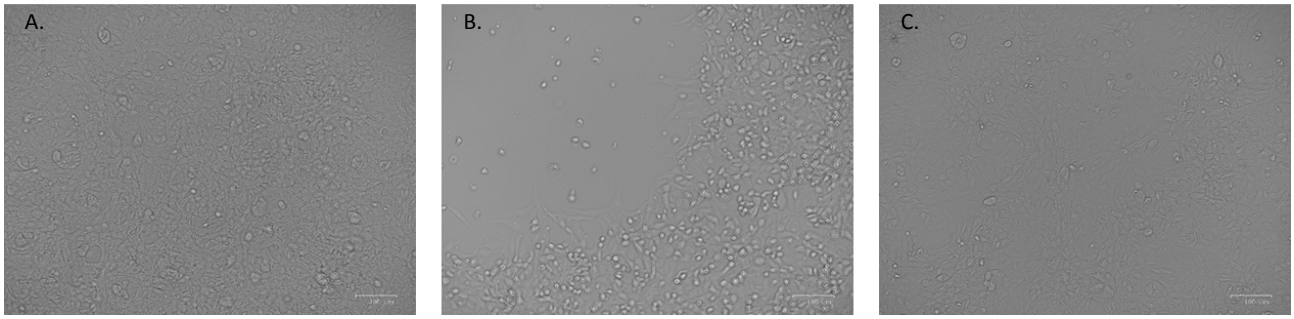

Figure 3. Analyses of virus induced cytopathic effect. (A) No cytopathic effect was observed in uninfected cultured VeroE6 monolayers maintained in 50mJ/cm^2 UV-treated complete medium for 72 hours. (B) In vitro infection of SARS-CoV-2 (5 MOI) UV-C untreated VeroE6 cells resulted in an evident cytopathic effect. (C) SARS-CoV-2 irradiation with 3.7 mJ/cm^2 UV-C rescued the cytopathic effect induced by UV-C untreated virus.

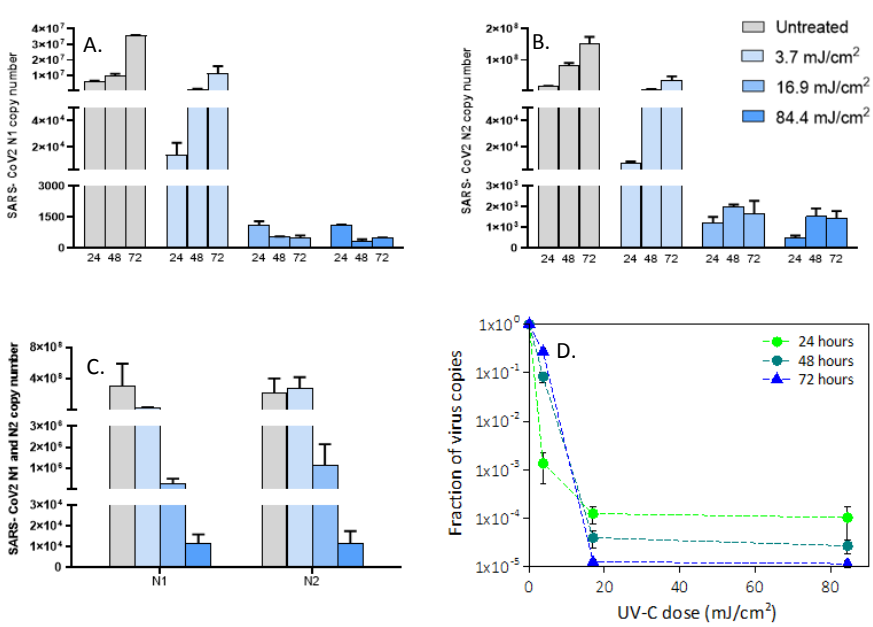

Figure 4. Viral replication of UV-irradiated SARS-CoV-2 (1000 MOI) virus in in vitro VeroE6 cells. Vero E6 cells were infected with UV-C irradiated SARS-CoV-2 virus at a MOI of 1000. Culture supernatants were harvested at the indicated times (24, 48 and 72 hours) and virus titers were measured (Panel A, B) by absolute copy number quantification (Real-Time PCR). Viral replication was assessed even on cell lysate harvested at the end of cell cultures (72 hours) (Panel C). All cell culture conditions were seeded in duplicate. Panel D reports the plots of the measured virus copies normalized at the untreated sample in the different conditions. For descriptive purposes, mean values and whiskers representing the observed half-ranges are shown.

Using a high viral input (MOI=1000), the two-way ANOVA confirmed that all the tree UV doses analysed resulted in a significant suppression of viral replication for both N1 (3.7 mJ/cm^2: p= 0.008455; 16.9 mJ/cm^2: p=0.004216; and 84.4 mJ/cm^2: p=0.000202) and N2 copies (3.7 mJ/cm^2: p= 6.43E-05; 16.9 mJ/cm^2:

119 p=1.68E-05; and 84.4 mJ/cm^2: p=1.68E-05)(Figure 4). Notably, a different course of infection was observed,
120 in which the inhibitory effect was not accompanied by viral suppression for the UV-C dose of 3.7 mJ/cm^2
121 (Figure 4, panel A, B and D). Indeed, a relevant reduction in N1 e N2 copy numbers was observed in a UV-C
122 dose-dependent manner as early as 24 hours (by a factor of 10^3 at 3.7 mJ/cm^2 and 10^4 at 16.9 mJ/cm^2,
123 Figure 4, panel A, B and D), but longer culture times resulted in an increase in N1 and N2 copy numbers for
124 the UV-C dose of 3.7 mJ/cm^2. This indicates that the residual viral input left by the 3.7 mJ/cm^2 was able to
125 replicate and suffucient to generate an effective infection. This is not the case in cultures exposed to
126 higher UV-C doses, as no replication could be detected in these conditions. All the results were further
127 confirmed by 2-ANOVA statistical analyses performed on viral replication at intracellular level (3.7 mJ/cm^2
128 vs. Untreated: N1, p=0.008455; N2: p=6.43E-05; 16.9 mJ/cm^2 vs. Untreated: N1, p=0.004216; N2: p=1.68E-
129 05; 84.4 mJ/cm^2 vs. Untreated: N1, p=0.004216; N2: p=1.68E-05) (Figure 1, panel C; Figure 2, panel C;
130 Figure 4, panel C).
131 We compared our results with data available in the literature and observed that our inactivating dose is
132 much smaller than that reported in Heilingloh et al.[26] (1000 mJ/cm^2 for the complete inactivation). This
133 discrepancy is likely to be the consequence of the UV-C absorption by the medium used in Heilingloh et al,
134 which has a 4-fold higher thickness compared to the one used in our experiments. This possibility is
135 supported by the observation that 200 mJ/cm^2 of UV-A, which is not absorbed by the medium, was
136 sufficient to reduce viral replication of 1-log. As UV-A light is significantly less efficient (order of
137 magnitudes) than UV-C, the reported UV-C inactivating dose (100mJ/cm2) seems to be questionable.
138 Two other papers measured the effect of UV-C light on SARS-CoV-2. In Ruetalo et al.[25], the illumination of
139 254 nm light was employed on a dried sample of SARS-CoV-2. Complete inactivation was obtained with 20
140 mJ/cm^2, a value greater than ours, but in the same range. It has to be underlined that in the dried film a
141 shielding effect by the organic component present in the liquid can occur, reducing the efficiency of the UV-
142 C light. This was shown by Ratnesar-Shumate et al.[28] , who demonstrated that the dose required to obtain a
143 similar degree of viral inactivation was twice in dried samples from gMEM compared to the ones
144 resuspended in simulated saliva. Notably, the two mediums differ for their composition, mainly in terms of
145 protein and solid percentage, with higher values for the gMEM.

146 Inagaki et al. used a 285 nm UV LED and showed that a dose of about 38 mJ/cm^2 was sufficient to
147 completely inactivate SARS-CoV-2. This dose is greater compared to the one we established ; this
148 discrepancy can be explained by the observation that the 285 nm is less efficient than the 254 nm
149 wavelength[24]. Finally, in an elegant study Storm et al.[27] compared the virucidal effect of UV-C in wet and
150 dry systems. Results were based on the use of a very small volume of viral stock in DMEM (5 μl) and
151 showed that a dose of 3.4 mJ/cm^2 inactivated wet samples, whereas a dose that twice as high was needed
152 in dried samples. These results are comparable to the ones herein, and the shielding effect in dried samples
153 is almost evident. Such comparisons show how the experimental conditions adopted significantly impact on
154 the definition of the dose of UV-C resulting in virus inactivation. It is therefore crucial to accurately describe
155 all the details of the experiments to perform a reliable comparison.
156 In conclusion, we report the results of a highly controlled experimental model that allowed us to identify
157 the UV-C radiation dose sufficient to inactivate SARS-CoV-2. The response depends on both the UV-C dose
158 and the virus concentration. Indeed, for virus concentrations typical of low-level contaminated closed
159 environment and sputum of COVID-19 infected patients, a very small dose of less than 4 mJ/cm^2 was
160 enough to achieve full inactivation of the virus. Even at the highest viral input concentration (1000 MOI),
161 viral replication was totally inactivated with a dose $\geq$16.9 mJ/cm$^{2.}$ These results show how the SARS-CoV-2
162 is extremely sensitive to UV-C light and they are important to allow the proper design and development of
163 efficient UV based disinfection methods to contain SARS-CoV-2 infection.
164

165 **Methods**

166 ***In vitro* SARS-CoV-2 infection assay**

167 3 x 10^5 VeroE6 cells were cultured in DMEM (ECB7501L, Euroclone, Milan, Italy) with 2 % FBS medium, with
168 100 U/ml penicillin and 100 μg/ml streptomycin, in a 24-well plate one day before viral infection assay.
169 SARS-CoV-2 (Virus Human 2019-nCoV strain 2019- nCoV/Italy-INMI1, Rome, Italy) at a multiplicity of
170 infection (MOI) of 1000, 5 and 0.05 were treated with different doses of UV-C radiation (see the dedicated
171 section) before inoculum into VeroE6 cells. UV-C-untreated virus served as positive controls. Cell cultures

172 were incubated with the virus inoculum in duplicate for three hours at 37°C and 5% CO_2. Then, cells were
173 rinsed three times with warm PBS, replenished with the appropriate growth medium and observed daily for
174 cytopathic effect. Viral replication in culture supernatants was assessed by an Integrated Culture-
175 polymerase chain reaction (C-RT-PCR) method[30] at 24, 48, and 72 hours post-infection (hpi) while infected
176 cells were harvested for RNA collection at 72 hpi. Cell cultures from SARS-CoV-2 at 0.05 MOI were
177 harvested 6 days post infection. RNA was extracted from VeroE6 cell culture supernatant and cell lysate by
178 the Maxwell® RSC Instrument with Maxwell® RSC Viral Total Nucleic Acid Purification Kit (Promega,
179 Fitchburg, WI, USA), quantified by the Nanodrop 2000 Instrument (Thermo Scientific) and purified from
180 genomic DNA with RNase-free DNase (RQ1 DNase; Promega). One microgram of RNA was reverse
181 transcribed into first-strand cDNA in a 20-µl final volume as previously described[31,32].

182 Real-time PCR was performed on a CFX96 (Bio-Rad, CA, USA) using the 2019-nCoV CDC qPCR Probe Assay
183 emergency kit (IDT, Iowa, USA), which targets two regions (N1 and N2) of the nucleocapsid gene of SARS-
184 CoV-2. Reactions were performed according to the following thermal profile: initial denaturation (95°C, 10
185 min) followed by 45 cycles of 15 s at 95°C (denaturation) and 1 min at 60°C (annealing-extension).

186 Viral copy quantification was assessed by creating a standard curve from the quantified 2019-nCoV_N
187 positive Plasmid Control (IDT, Iowa, USA).

188 **UV illumination test**

189 The illumination of the virus solution was conducted using a low-pressure mercury lamp mounted in a
190 custom designed holder, which consist in a box with a circular aperture 50 mm in diameter placed at
191 approximately 220 mm from the source. The aperture works as a spatial filter to make the illumination of
192 the area behind more uniform. A mechanical shutter is also present to start the illumination process. The
193 plate is placed 30 mm below the circular aperture and a single dwell (34.7 mm in diameter), centered in
194 respect to the 50 mm aperture, has been irradiated from the top. The dwell was filled with 0.976 ml of the
195 virus suspended in Dulbecco's Modified Eagle's Medium (DMEM) in order to have a 1 mm thick liquid layer.
196 After the irradiation, the sample was treated as described in the previous section.

The intensity of the lamp and its spectral properties have been measured using an Ocean Optics HR2000+ spectrometer (Ocean Optics Inc., Dunedin, USA). The HR2000+ spectrometer was calibrated against a reference deuterium–halogen source (Ocean Optics Inc. Winter Park, Winter Park, Florida) and in compliance with National Institute of Standards and Technology (NIST) practices recommended in NIST Handbook 150-2E, Technical guide for Optical Radiation Measurements. The last calibration was performed in March 2019. The detector of our spectrometer is a high-sensitivity 2048-element Charge-Coupled Device (CCD) array from Sony. The spectral range is 200–1100 nm with a 25 µm wide entrance slit and an optical resolution of 1.4 nm (FWHM). The cosine-corrected irradiance probe, model CC-3-UV-T, is attached to the tip of a 1 m long optical fibre and couples to the spectrometer. The intensity of the lamp has been measured by positioning the spectrometer in five positions: in the center and at the ends of a 20 mm cross arm after a warming up time of 30 s. The spectra in the five positions are reported in Figure 5 (Panel A) together with a scheme of the dwell and illuminated area.

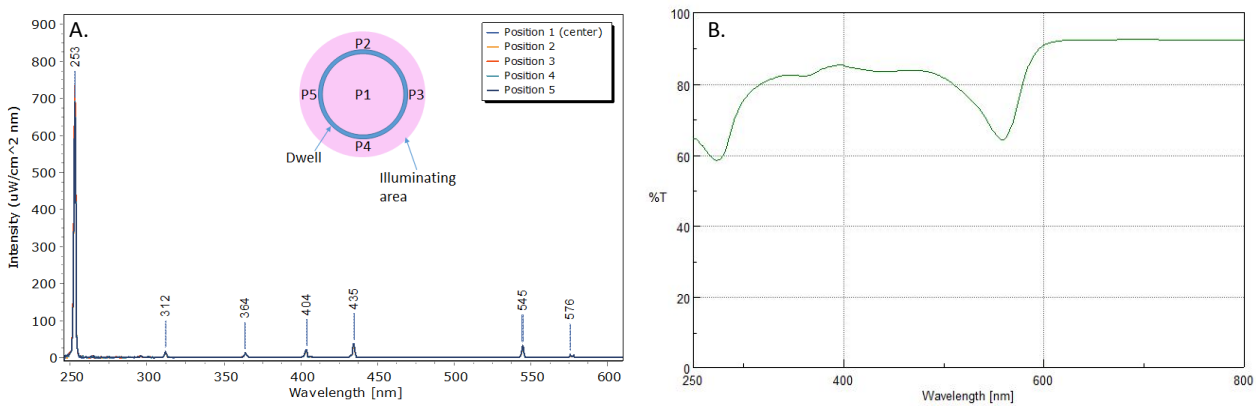

Figure 5. *Mercury lamp spectrum measured in the five positions (Panel A). Inset: scheme of the illuminated dwell and the measuring position. UV-vis transmission spectrum of the Dulbecco's Modified Eagle's Medium (DMEM) in a 1 mm quartz cuvette (Panel B).*

As expected, the emission is dominated by the UV-C line (Figure 5, Panel A) and its intensity was uniform in the area with an average value of 1.082 mW/cm^2. The stability of the lamp was evaluated in +/- 11E-3 mW/cm^2 during a 130 s measurement. According to this value, three exposure times were set: 5, 23 and 114 s (with an accuracy of 0.2s), which correspond to following doses: 5.4, 25.0, 123.4 mJ/cm^2. This is the nominal UV doses provided to the dwell, but we were interested in the effective doses (D_e) reaching the virus. It was necessary to calculate the effective irradiance (I_e). This step was performed considering both

218 the reflection losses at the air/water interface (R_w) and the Transmittance (T_s) of the DMEM solution at 254

219 nm (from the spectrum in figure 5, Panel B, considering the cuvette losses, T_s = 0 .70). It is important to

220 notice that the spectrum was measured in a quartz cuvette (1 mm thick) by means of a Jasco V770

221 spectrophotometer and this thickness was the same of the solution in the dwell during the UV irradiation

222 step.

223 The reflection loss was computed as follow:

224 $$\mathrm{R}_w = \frac{(\mathrm{n}_w - 1)^2}{(\mathrm{n}_w + 1)^2} \quad (1)$$

225 Where n_w = 1.375 is the refractive index of water at 254 nm. Then, I_e was calculated:

226 $$I_e = I_n(1 - R_w) \times T_s \quad (2)$$

227 The final transmission of the DMEM solution was equal to 0.68 and the corresponding effective doses were

228 derived simply multiplying I_e by the exposure time.

229 According to this value, the effective doses provided to the viruses were: 3.7±0.15, 16.9±0.2 and 84.4±0.9

230 mJ/cm^2. We have to notice that we are neglecting here the absorption of the virus at this wavelength and

231 the possible scattering. Such approximations are valid considering the relative low concentration of the

232 virus and small thickness of the layer (the solution appeared fully transparent).

233 **Statistical analyses**

234 To assess the effect of the different UV-C doses on N1 and N2 copy numbers, two-way ANOVAs were

235 performed. For the analysis of intracellular N1 and N2 doses in the supernatant, UV-C dose and MOI

236 represented the dependent variables, while for the analysis of N1 and N2 in the supernatant, different

237 analyses were performed for individual MOI, using UV-C dose and time as dependent variables.

238

239

240

241

242

243

244

245

246

247 **References**

248 1. Zhu, N. *et al.* A Novel Coronavirus from Patients with Pneumonia in China, 2019. *N. Engl. J. Med.*
249 **382**, 727–733 (2020).

250 2. Cobey, S. Modeling infectious disease dynamics. *Science* **368**, 713–714 (2020).

251 3. Jarvis, M. C. Aerosol Transmission of SARS-CoV-2: Physical Principles and Implications. *Front. Public*
252 *Heal.* **8**, 590041 (2020).

253 4. Tang, S. *et al.* Aerosol transmission of SARS-CoV-2? Evidence, prevention and control. *Environ. Int.*
254 **144**, 106039 (2020).

255 5. van Doremalen, N. *et al.* Aerosol and Surface Stability of SARS-CoV-2 as Compared with SARS-CoV-1.
256 *N. Engl. J. Med.* **382**, 1564–1567 (2020).

257 6. Chin, A. W. H. *et al.* Stability of SARS-CoV-2 in different environmental conditions. *The Lancet*
258 *Microbe* **1**, e10 (2020).

259 7. Aboubakr, H. A., Sharafeldin, T. A. & Goyal, S. M. Stability of SARS-CoV-2 and other coronaviruses in
260 the environment and on common touch surfaces and the influence of climatic conditions: A review.
261 *Transbound. Emerg. Dis.* 10.1111/tbed.13707 (2020) doi:10.1111/tbed.13707.

262 8. Pirnie, M., Linden, K. G. & Malley, J. P. J. Ultraviolet disinfection guidance manual for the final long
263 term 2 enhanced surface water treatment rule. *Environ. Prot.* **2**, 1–436 (2006).

264 9. Reed, N. G. The history of ultraviolet germicidal irradiation for air disinfection. *Public Health Rep.*
265 **125**, 15–27 (2010).

266 10. Kovalski, W. *Ultraviolet germicidal irradiation handbook: UVGI for air and surface disinfection*.
267 (Springer Science & Business Media, 2010).

268 11. Darnell, M. E. R., Subbarao, K., Feinstone, S. M. & Taylor, D. R. Inactivation of the coronavirus that
269 induces severe acute respiratory syndrome, SARS-CoV. *J. Virol. Methods* **121**, 85–91 (2004).

270 12. Raeiszadeh, M. & Adeli, B. A Critical Review on Ultraviolet Disinfection Systems against COVID-19
271 Outbreak: Applicability, Validation, and Safety Considerations. *ACS Photonics* **7**, 2941–2951 (2020).

272 13. Bosshard, F., Armand, F., Hamelin, R. & Kohn, T. Mechanisms of Human Adenovirus Inactivation by
273 Sunlight and UVC Light as Examined by Quantitative PCR and Quantitative Proteomics. *Appl. Environ.*
274 *Microbiol.* **79**, 1325 – 1332 (2013).

275 14. Nishisaka-Nonaka, R. *et al.* Irradiation by ultraviolet light-emitting diodes inactivates influenza a
276 viruses by inhibiting replication and transcription of viral RNA in host cells. *J. Photochem. Photobiol.*
277 *B Biol.* **189**, 193–200 (2018).

278 15. Araud, E., Fuzawa, M., Shisler, J. L., Li, J. & Nguyen, T. H. UV Inactivation of Rotavirus and Tulane
279 Virus Targets Different Components of the Virions. *Appl. Environ. Microbiol.* **86**, e02436-19 (2020).

280 16. Qiao, Z. & Wigginton, K. R. Direct and Indirect Photochemical Reactions in Viral RNA Measured with
281 RT-qPCR and Mass Spectrometry. *Environ. Sci. Technol.* **50**, 13371–13379 (2016).

282 17. Wigginton, K. R. & Kohn, T. Virus disinfection mechanisms: the role of virus composition, structure,
283 and function. *Curr. Opin. Virol.* **2**, 84–89 (2012).

284 18. Lytle, C. D. & Sagripanti, J.-L. Predicted Inactivation of Viruses of Relevance to Biodefense by Solar
285 Radiation. *J. Virol.* **79**, 14244 LP – 14252 (2005).

286 19. Walker, C. M. & Ko, G. Effect of Ultraviolet Germicidal Irradiation on Viral Aerosols. *Environ. Sci.*
287 *Technol.* **41**, 5460–5465 (2007).

288 20. McDevitt, J. J., Rudnick, S. N. & Radonovich, L. J. Aerosol susceptibility of influenza virus to UV-C
289 light. *Appl. Environ. Microbiol.* **78**, 1666–1669 (2012).

290 21. Calgua, B. *et al.* UVC Inactivation of dsDNA and ssRNA Viruses in Water: UV Fluences and a qPCR-
291 Based Approach to Evaluate Decay on Viral Infectivity. *Food Environ. Virol.* **6**, 260–268 (2014).

292 22. Eickmann, M. *et al.* Inactivation of three emerging viruses – severe acute respiratory syndrome
293 coronavirus, Crimean–Congo haemorrhagic fever virus and Nipah virus – in platelet concentrates by
294 ultraviolet C light and in plasma by methylene blue plus visible light. *Vox Sang.* **115**, 146–151 (2020).

295 23. Duan, S.-M. *et al.* Stability of SARS Coronavirus in Human Specimens and Environment and Its
296 Sensitivity to Heating and UV Irradiation. *Biomed. Environ. Sci.* **16**, 246–255 (2003).

297 24. Inagaki, H., Saito, A., Sugiyama, H., Okabayashi, T. & Fujimoto, S. Rapid inactivation of SARS-CoV-2
298 with Deep-UV LED irradiation. *Emerg. Microbes Infect.* **9**, 1744–1747 (2020).

299 25. Ruetalo, N., Businger, R. & Schindler, M. Rapid and efficient inactivation of surface dried SARS-CoV-2
300 by UV-C irradiation. *bioRxiv* 2020.09.22.308098 (2020).

301 26. Heilingloh, C. S. *et al.* Susceptibility of SARS-CoV-2 to UV irradiation. *Am. J. Infect. Control* **48**, 1273–
302 1275 (2020).

303 27. Storm, N. *et al.* Rapid and complete inactivation of SARS-CoV-2 by ultraviolet-C irradiation. *Sci. Rep.*
304 **10**, 22421 (2020).

305 28. Ratnesar-Shumate, S. *et al.* Simulated Sunlight Rapidly Inactivates SARS-CoV-2 on Surfaces. *J. Infect.*
306 *Dis.* **222**, 214–222 (2020).

307 29. Wölfel, R. *et al.* Virological assessment of hospitalized patients with COVID-2019. *Nature* **581**, 465–
308 469 (2020).

309 30. Reynolds, K. A. Integrated Cell Culture/PCR for Detection of Enteric Viruses in Environmental
310 Samples BT - Public Health Microbiology: Methods and Protocols. in (eds. Spencer, J. F. T. & Ragout
311 de Spencer, A. L.) 69–78 (Humana Press, 2004). doi:10.1385/1-59259-766-1:069.

312 31. Saulle, I. *et al.* Endoplasmic Reticulum Associated Aminopeptidase 2 (ERAP2) Is Released in the
313 Secretome of Activated MDMs and Reduces in vitro HIV-1 Infection. *Front. Immunol.* **10**, 1648
314 (2019).

315 32. Ibba, S. V *et al.* Analysing the role of stat3 in HIV-1 infection. *Journal of Biological Regulators and*
316 *Homeostatic Agents* **33** 1635–1640 (2019).

317

318

319 **Acknowledgements**

320 This research was partially supported by a grant from Falk Renewables and it has been carried out in the
321 context of the activities promoted by the Italian Government and in particular, by the Ministries of Health
322 and of University and Research, against the COVID-19 pandemic. Authors are grateful to INAF's President,
323 Prof. N. D'Amico, for the support and for a critical reading of the manuscript.

Author Contribution

P.G., L.L. E.R. and A.Z. designed and produced the illumination system; A.C., C.C. and M.L. performed the lamp calibration; A.B. performed the lamp setup and lamp dosimetry, wrote the main manuscript; M.B. performed biological experiments, analyzed the data, wrote the main manuscript; C.F., I.S. designed and performed some biological tests; E.T, A.A. performed the statistical analysis; D.T. discussed the results; G.P. and M.C. supervised the study and review the manuscript.